Multifractality and Intermittency in the Solar Wind

Wiesław M. Macek

Faculty of Mathematics and Natural Sciences. College of Sciences,
Cardinal Stefan Wyszyński University, Dewajtis 5, 01-815 Warsaw, Poland;
Space Research Centre, Polish Academy of Sciences,
Bartycka 18 A, 00-716 Warsaw, Poland
e-mail: macek@cbk.waw.pl, http://www.cbk.waw.pl/∼macek

NLW-6 2006, 9–13 October 2006, Fukuoka, Japan

Abstract

The question of multifractality is of great importance because it allows us to look at intermittent turbulence in the solar wind. Starting from Richardson's version of turbulence, many authors try to recover the observed scaling exponents, using various models of the turbulence cascade for the dissipation rate. The multifractal spectrum has been investigated with Voyager (magnetic field) data in the outer heliosphere and with Helios (plasma) data in the inner heliosphere. We have shown that the multifractal spectrum of the solar wind attractor is consistent with that for the multifractal measure on the self-similar weighted baker's map with two parameters describing uniform compression and natural invariant probability measure on the attractor of the system. In order to further quantify that multifractality, we thus consider generalized two-scale weighted Cantor set. We investigate the resulting multifractal spectrum depending on scaling parameters and the probability measure parameter, especially for asymmetric scaling. We hope that this model could be a useful tool for analysis of the intermittent turbulence in space plasmas. In particular, taking two different scales for eddies in the cascade, one obtains a more general situation than in the usual p-model for fully developed turbulence.

Within the complex dynamics of the solar wind's fluctuating plasma parameters, there is a detectable, hidden order described by a chaotic strange attractor which has a multifractal structure.

Plan of Presentation

1. Introduction
   - Fractal Analysis Basics
   - Importance of Multifractality
2. Solar Wind Data
   - Noise Reduction
   - Attractor Reconstruction
3. Methods for Multifractality
   - Generalized Dimensions and Entropies
   - Multifractal Spectrum
4. Results and Discussion
   - Dimensions and Multifractality
   - Generalized Cantor Set Model for Solar Wind Turbulence
5. Conclusions

Fractals

A **fractal** is a rough or fragmented geometrical object that can be subdivided in parts, each of which is (at least approximately) a reduced-size copy of the whole. Fractals are generally *self-similar* and independent of scale (fractal dimension).

A **multifractal** is a set of intertwined fractals. Self-similarity of multifractals is scale dependent (spectrum of dimensions).

Chaos and Attractors

CHAOS ($\chi\alpha o\varsigma$) is

- APERIODIC long-term behavior
- in a DETERMINISTIC system
- that exhibits SENSITIVITY TO INITIAL CONDITIONS.

A positive finite Lyapunov exponent (metric entropy) implies chaos.

An **ATTRACTOR** is a *closed* set A with the properties:

1. A is an INVARIANT SET:
   any trajectory $\mathbf{x}(t)$ that start in A stays in A for ALL time t.
2. A ATTRACTS AN OPEN SET OF INITIAL CONDITIONS:
   there is an open set U containing A ($\subset U$) such that if $\mathbf{x}(0) \in U$, then the distance from $\mathbf{x}(t)$ to A tends to zero as $t \to \infty$.
3. A is MINIMAL:
   there is NO proper subset of A that satisfies conditions 1 and 2.

The question of multifractality is of great importance because it allows us to look at intermittent turbulence in the solar wind (e.g., Marsch and Tu, 1997; Bruno et al., 2001). Starting from Richardson's version of turbulence, many authors try to recover the observed scaling exponents, using various models of the turbulence cascade for the dissipation rate. The multifractal spectrum has been investigated with Voyager (magnetic field) data in the outer heliosphere (e.g., Burlaga, 1991, 2001) and with Helios (plasma) data in the inner heliosphere (e.g., Marsch et al., 1996).

A direct determination of the multifractal spectrum from the data is known to be a difficult problem. Indication for a chaotic attractor in the slow solar wind has been given by Macek (1998) and Macek and Redaelli (2000). In particular, Macek (1998) has calculated the correlation dimension of the reconstructed attractor in the solar wind and has provided tests for this measure of *complexity* including statistical surrogate data tests (Theiler et al., 1992). Further, Macek and Redaelli (2000) have shown that the Kolmogorov entropy of the attractor is *positive* and finite, as it holds for a *chaotic* system.

We have extended our previous results on the dimensional time series analysis (Macek, 1998). Namely, we have applied the technique that allows a realistic calculation of the generalized dimensions of the solar wind flow directly from the cleaned experimental signal by using the Grassberger and Procaccia method. The resulting spectrum of dimensions shows the multifractal structure of the solar wind in the inner heliosphere (Macek et al., 2005, 2006). Using a short data sample, we first demonstrate the influence of noise on these results and show that noise can efficiently be reduced by a singular-value decomposition filter (Macek, 2003, 2003). Using a longer sample we have shown that the multifractal spectrum of the solar wind attractor reconstructed in the phase space is consistent with that for the multifractal measure on the self-similar weighted baker's map (Macek et al., 2005) and, in particular, with the weighted Cantor set (Macek et al., 2006).

- W. M. Macek, Physica D **122**, 254–264 (1998).
- W. M. Macek and S. Redaelli, Phys. Rev. E **62**, 6496–6504 (2000).
- W. M. Macek, Multifractality and chaos in the solar wind, in *Experimental Chaos*, edited by S. Boccaletti, B. J. Gluckman, J. Kurths, L. M. Pecora, and M. L. Spano, American Institute of Physics, New York, 2002, Vol. 622, pp. 74–79.
- W. M. Macek, The multifractal spectrum for the solar wind flow, in *Solar Wind 10*, edited by M. Velli, R. Bruno, F. Malara, American Institute of Physics, New York, 2003, vol. 679, pp. 530–533.
- W. M. Macek, R. Bruno, G. Consolini, Generalized dimensions for fluctuations in the solar wind, Phys. Rev. E **72**, 017202 (2005).
- W. M. Macek, R. Bruno, G. Consolini, Testing for multifractality of the slow solar wind, Adv. Space Res. **37**, 461-466 (2006).
- W. M. Macek, Modeling multifractality of the solar wind, Space Sci. Rev. **122**, 329–337 (2006).

In order to further quantify that multifractality, we thus consider two-scale weighted Cantor set. We investigate the resulting multifractal spectrum depending on scaling parameters and the probability measure parameter, especially for asymmetric scaling. We hope that this model could be a useful tool for analysis of the intermittent turbulence in space plasmas. In particular, taking two different scales for eddies in the cascade, one obtains a more general situation than in the usual *p*-model for fully developed turbulence.

Thus our results provide direct supporting evidence that the *complex* solar wind is likely to have multifractal structure. In this way, we have further supported our previous conjecture that trajectories describing the system in the inertial manifold of phase space asymptotically approach the attractor of low-dimension. One can expect that the attractor in the low-speed solar wind plasma should contain information about the dynamic variations of the coronal streamers. It is also possible that it represents a structure of the time sequence of near-Sun coronal fine-stream tubes (see, Macek, 1998, 2006), and references therein.

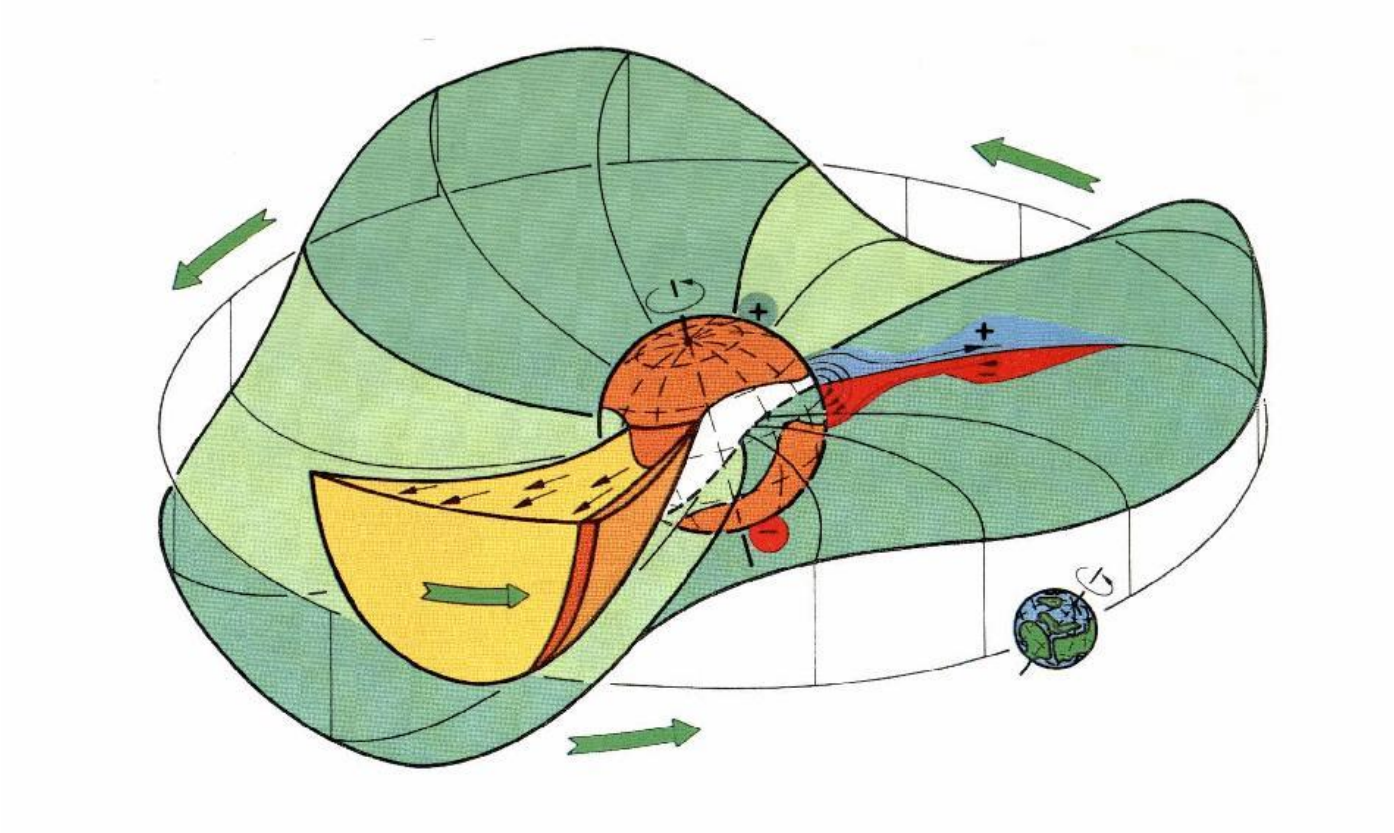

A schematic model of the solar wind ”ballerina”: the Sun’s two hemispheres are separated by a neutral layer of a form reminiscent of a ’ballerina’s skirt’. In the inner heliosphere the solar wind streams are of two forms called the slow (≈ 400 km s^{-1}) and fast (≈ 700 km s^{-1}). The fast wind is associated with coronal holes and is relatively uniform and stable, while the slow wind is quite variable, taken from (Schwenn and Rosenbauer, 1984).

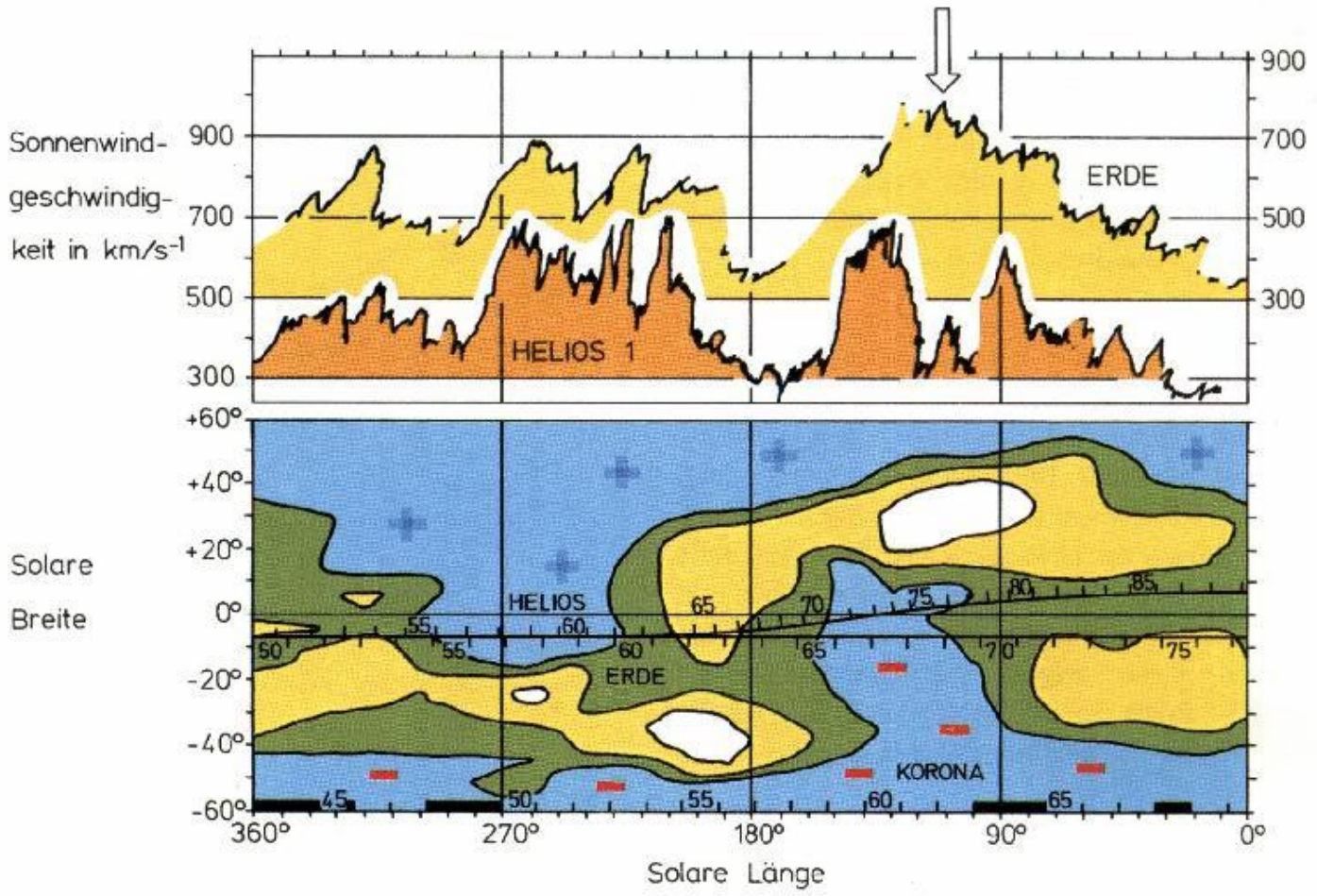

Structures in the solar wind and their sources in the corona (solar map), taken from (Schwenn and Rosenbauer, 1984).

Helios Spacecraft

Orbits

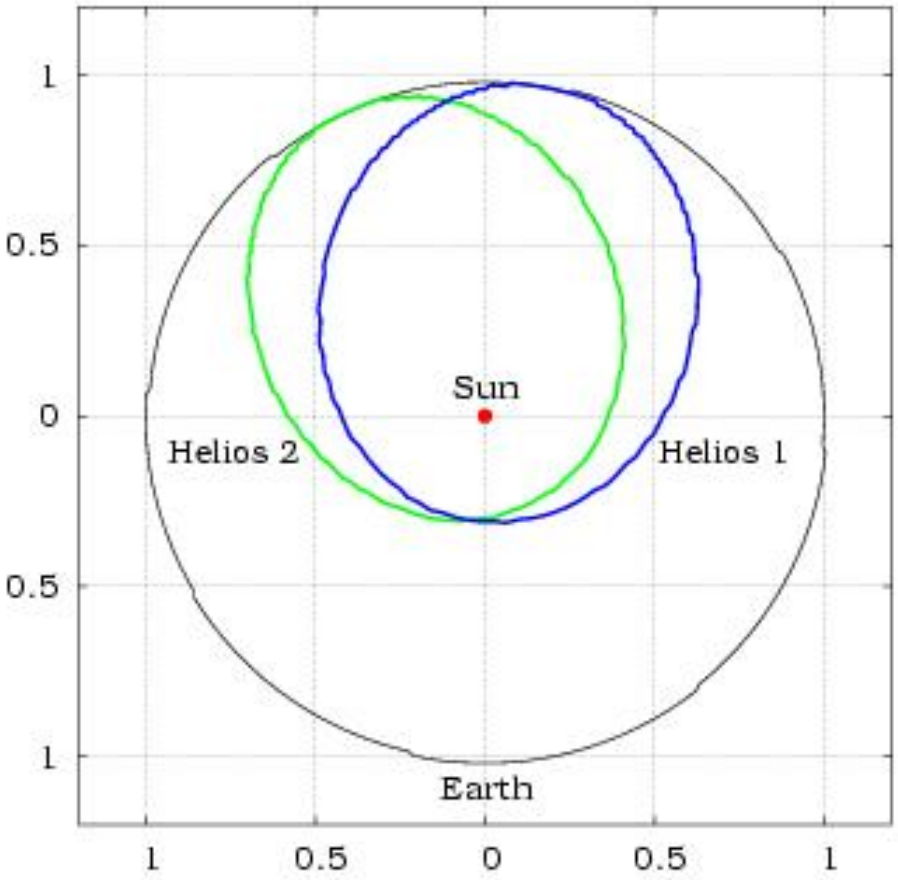

Data

No	Year	From (DOY)	To (DOY)	Distance from the Sun (AU)
I	1977	116	121	0.32
II	1977	348	357	0.84

Sampling time: 40.5 s

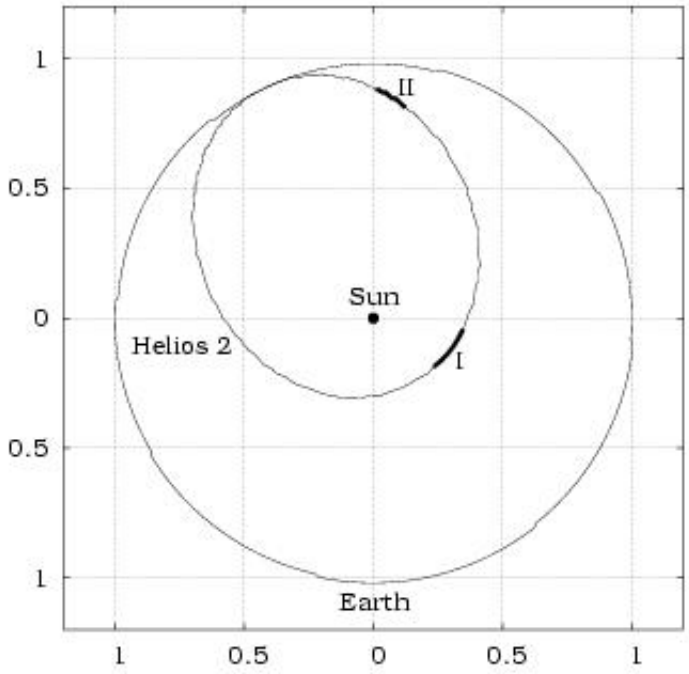

Alfvénic Velocity

Sound velocity: $c_s^2 = \gamma \frac{p}{\rho}$

Magnetic field pressure: $p = \frac{B^2}{8\pi}$

Adiabatic exponent: $\gamma = \frac{f+2}{f} = 2 \quad f = 2$

Alfvénic velocity: $v_A = \frac{B}{\sqrt{4\pi\rho}}$

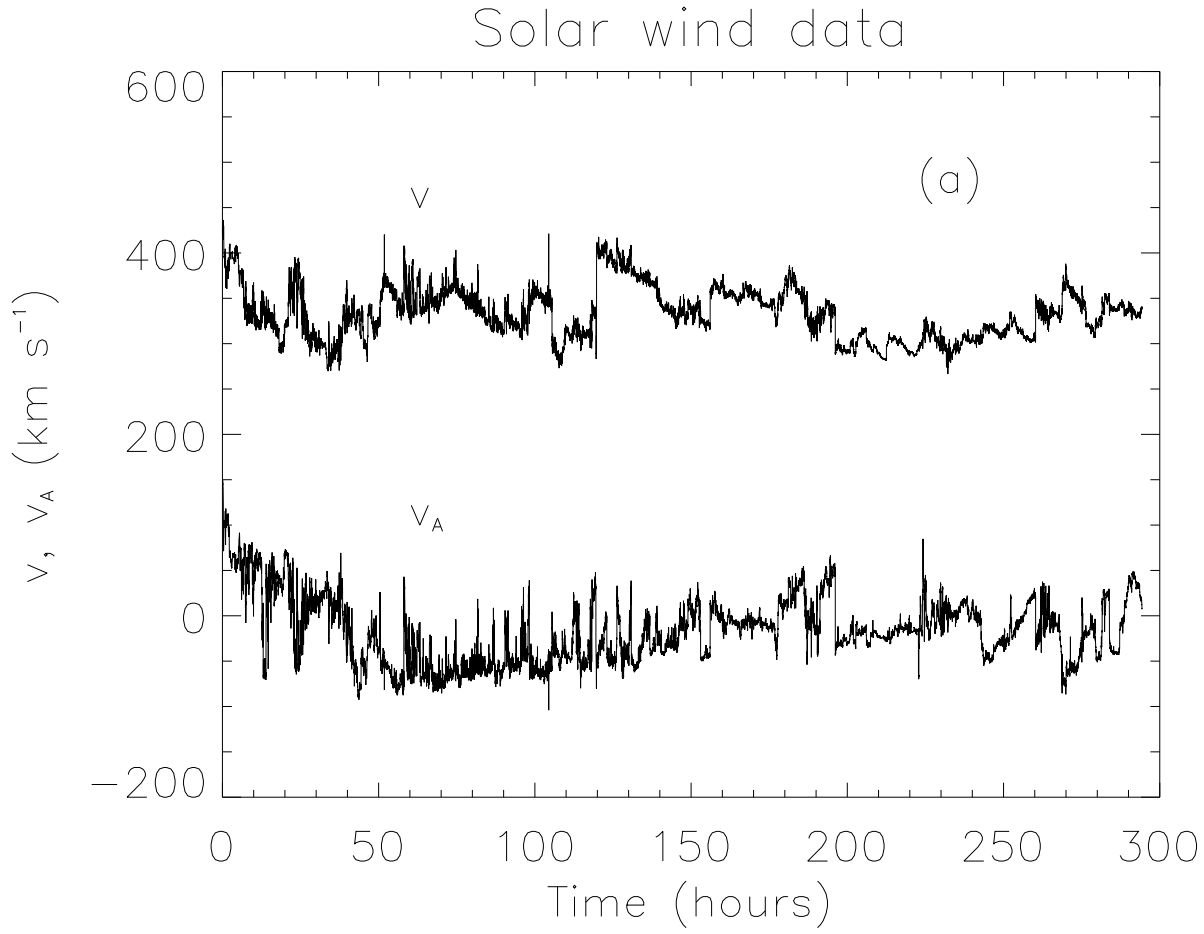

Fig. 1. (a) The raw data of the radial flow velocity with Alfvénic velocity, v and v_A, observed by the Helios 2 spacecraft in 1977 from 116:00 to 121:21 (day:hour) at distances 0.3 AU, and from 348:00 to 357:00 at 0.9 AU from the Sun, taken from (Macek et al., 2005).

Singular-value Decomposition

The normalized vectors $\mathbf{X}(t_i) = [v(t_i), v(t_i+\tau), \ldots, v(t_i+(m-1)\tau)]$ in the embedding phase space of dimension m, where $i = 1, \ldots, n$, $n = N-(m-1)\tau$, number of vectors.

A is the $n \times m$ trajectory matrix $(n \geq m)$

$$A = \frac{1}{\sqrt{n}} \begin{pmatrix} \mathbf{X}(t_1) \\ \mathbf{X}(t_2) \\ \vdots \\ \mathbf{X}(t_n) \end{pmatrix}$$

Decomposition

The matrix $A_{ij} = v(t_i + (j-1)\tau) = UWV^T$, $j = 1, \ldots, m$,
$U - n \times m$ matrix with orthonormal columns, $(U^T U)_{ij} = \delta_{ij}$,
$V - m \times m$ orthonormal matrix, $(V^T V)_{ij} = (VV^T)_{ij} = \delta_{ij}$,
$W - m \times m$ diagonal matrix, $W_{ij} = \delta_{ij}\, w(j)$.

The projection of the original vectors onto the new orthogonal space:
$A \rightarrow A^{'} = AV = UW$
the matrix of eigenfunctions $\Psi^{'} = A^{'}W$ and $\Psi = U$.

Normalization, for a given m,

$$\xi_j = w^2(j)/(\sum_{k=1}^{m} w^2(k)) \tag{1}$$

is the variance of the j-th principal component;

Normalization of the eigenfunctions, $j = 1, \ldots, m$,

$$\frac{1}{n} \sum_{i=1}^{n} |\Psi^{'}_{ij}|^2 = {\xi_j}^2 \tag{2}$$

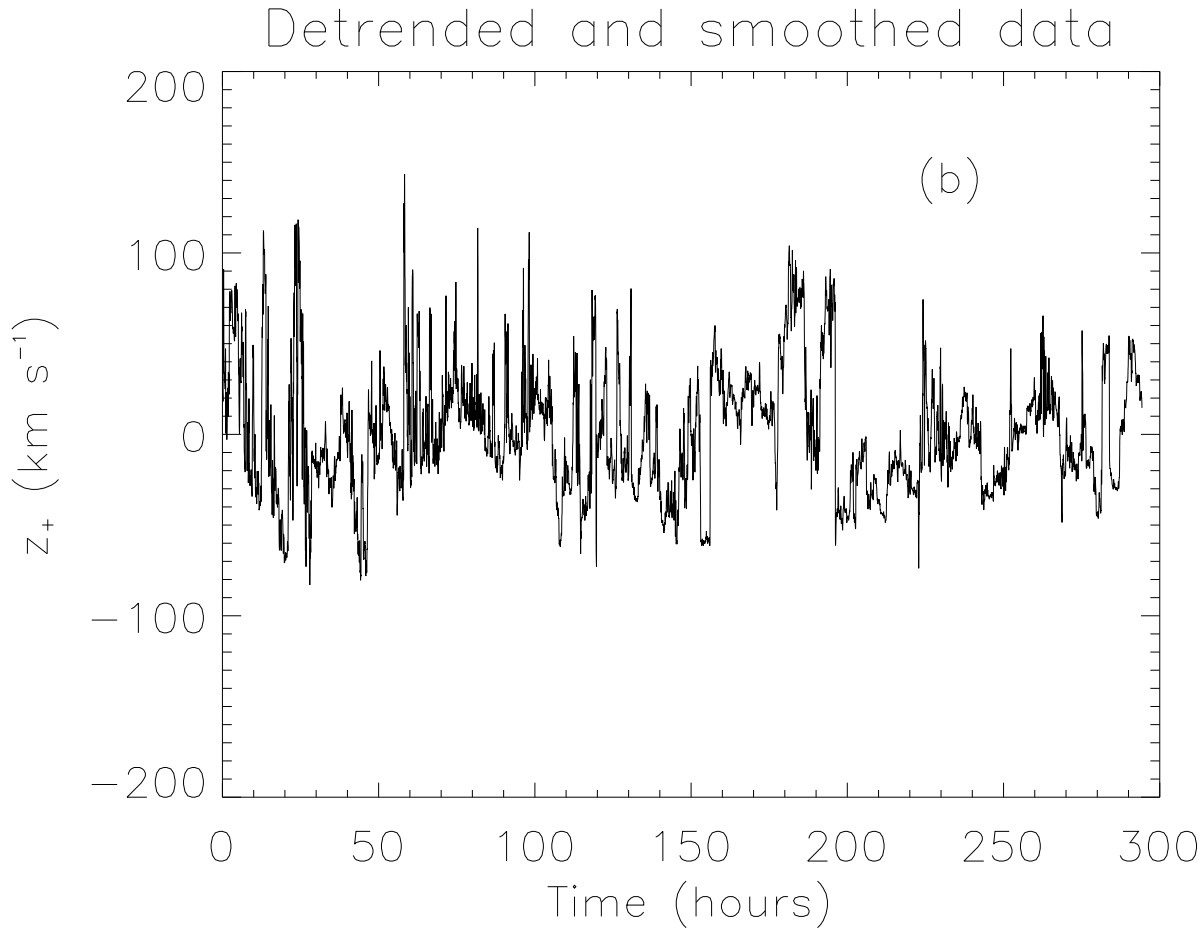

Fig. 1. (b) The Elsässer variable $z_+ = v \pm v_A$ for B_o pointing to/away from the Sun for the detrended and filtered data using singular-value decomposition with five largest eigenvalues, taken from (Macek et al., 2005).

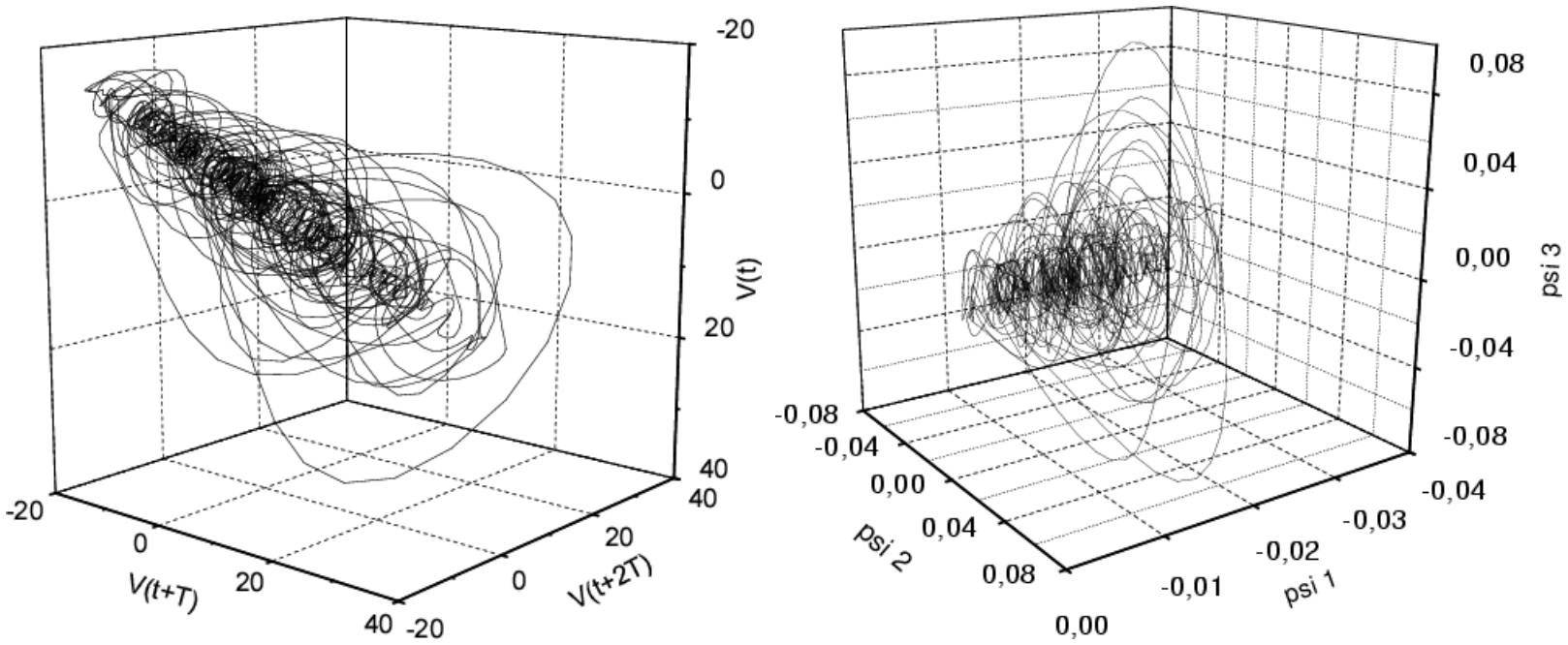

Fig. 2. The projection of the attractor onto the three-dimensional space, reconstructed from the detrended data, $T = 4\,\Delta t$, using (a) the moving average and also (b) the singular-value decomposition filters ($\Psi = U$), taken from (Macek, 1998).

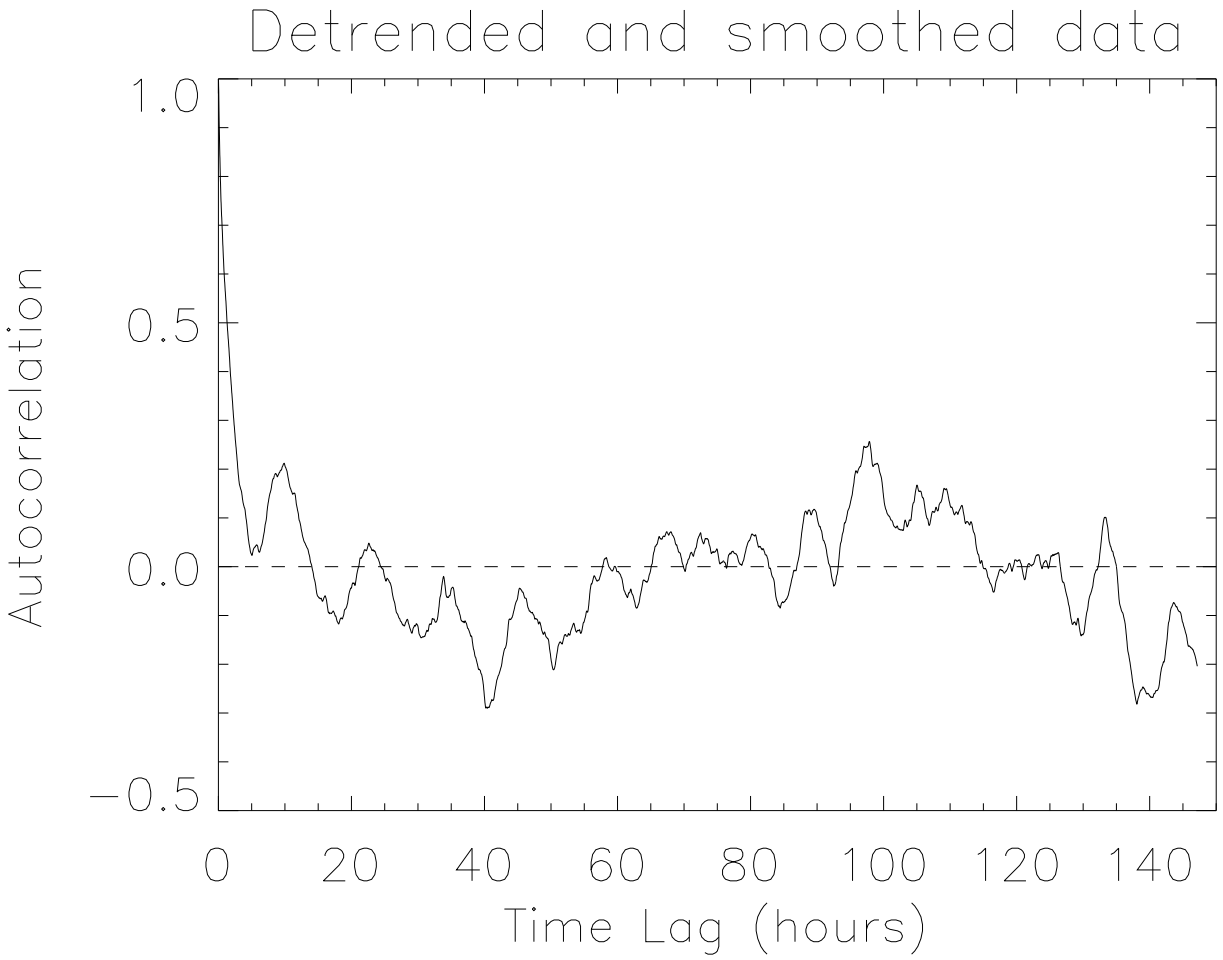

Fig. 3. The normalized autocorrelation function as a function of the time lag for the detrended and filtered data, taken from (Macek et al., 2006).

Method

Dimensions

The generalized dimensions of attractors are important characteristics of *complex* dynamical systems. Since these dimensions are related to frequencies with which typical orbits in phase space visit different regions of the attractors, they can provide information about dynamics of the systems. More precisely, one may distinguish a probability measure from its geometrical support, which may or may not have fractal geometry. Then, if the measure has different fractal dimensions on different parts of the support, the measure is multifractal. The modern technique of nonlinear time series analysis allows to estimate the multifractal measure directly from a single time series.

$M(r)$, number of hyperspheres of size r in the phase space needed to cover the attractor;
p_j, probability that a point from a time series falls in jth hypersphere;
the q-order function, $j = 1, \ldots, M$,

$$I_q(r) = \sum_{j=1}^{M} (p_j)^q, \tag{3}$$

the q-order generalized *dimension*

$$D_q = \frac{1}{q-1} \lim_{r \to 0} \frac{\ln I_q(r)}{\ln r} \tag{4}$$

Weighted average: $I_q(r) = \sum p_j (p_j)^{q-1} = \langle (p_j)^{q-1} \rangle$
the generalized average probability per hypersphere:
$\mu = \sqrt[q-1]{\langle (p_j)^{q-1} \rangle} \propto r^{D_q}$.

- $q = 0$, the capacity dimension, $I_0 = M$,

$$D_0 = \lim_{r \to 0} \frac{\ln M(r)}{\ln(1/r)} \tag{5}$$

- $q \to 1$, geometrical average, the information dimension

$$D_1 = \lim_{r \to 0} \frac{\sum (p_j \ln p_j)}{\ln r} \approx \frac{\langle \ln p_j \rangle}{\ln r} \tag{6}$$

- $q = 2$, arithmetic average, the correlation dimension

$$D_2 = \lim_{r \to 0} \frac{\ln \sum (p_j)^2}{\ln r} \approx \frac{\ln \langle p_j \rangle}{\ln r} \tag{7}$$

- $q = 3$, root-mean-square average

High order dimensions quantify the multifractality of the probability measure on the attractor.

In practice, for a given m and r,

$$p_j \simeq \frac{1}{n-2n_{\rm c}-1} \sum_{i=n_c+1}^{n} \theta(r- \mid \mathbf{X}(t_i)-\mathbf{X}(t_j) \mid) \tag{8}$$

with $\theta(x)$ being the unit step function; $\mathbf{X}(t_j)$ denotes one of $n = N-(m-1)\tau$ vectors in the m-dimensional embedding space,
$\mathbf{X}(t_i) = [v(t_i), v(t_i+\tau), \ldots, v(t_i+(m-1)\tau)]$,
τ, delay time, characteristic time of autocorrelation function.

$I_q(r)$ is equal to the generalized q-point correlation sum

$$C_{q,m}(r) \;=\; \frac{1}{n_{\rm ref}} \sum_{j=1}^{n_{\rm ref}} (p_j)^{q-1} \tag{9}$$

where $n_{\rm ref} = 5000$ is the number of reference vectors.

For large m and small r in the scaling region

$$C_{q,m}(r) \propto r^{(q-1)D_q} \exp(-m\tau K_q) \tag{10}$$

D_q and K_q are approximations of the limit $r \to 0$ in Eq. (4).
The average slope for $6 \le m \le 10$ is taken as $(q-1)D_q$.

Entropy

The q-order Kolmogorov *entropy*

$$K_q = \frac{1}{1-q} \lim_{r \to 0} \ln I_q(r) \tag{11}$$

is the rate of creation of information as a chaotic orbit evolves

$$K_2 \approx \frac{1}{3} \log_2 \left[\frac{C_m(r)}{C_{m+3}(r)} \right] \tag{12}$$

is the $q = 2$ entropy (base 2)
in the same units as $\lambda_{\max}$ (bits per data sample),
$8 \leq m \leq 10$.

the *chaotic* attractor:
at least one unstable direction (*positive* exponent),
the largest positive Lyapunov exponent, $\lambda_{\max}$ (using *Kantz* algorithm);
the Kolmogorov correlation ($q = 2$) entropy

$$K_2 \leq \sum \lambda_i \tag{13}$$

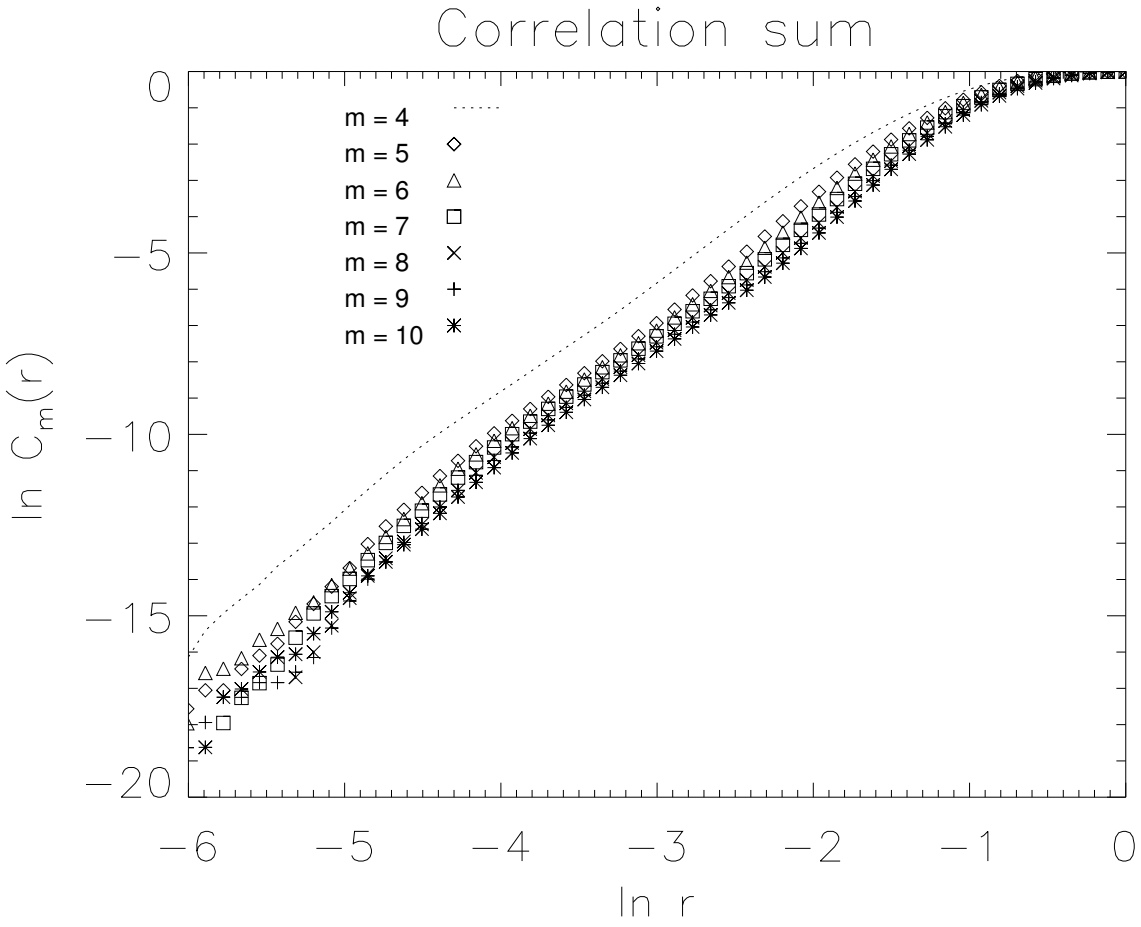

Fig. 4. The natural logarithm of the correlation sum $C_m(r)$ versus $\ln r$ (normalized), $q = 2$, obtained for the cleaned experimental signal is shown for various embedding dimensions: $m = 4$ (dotted curve), $m = 5$ (diamonds), 6 (triangles), 7 (squares), 8 (crosses), 9 (plus), and 10 (stars), (cf. Macek, 2002).

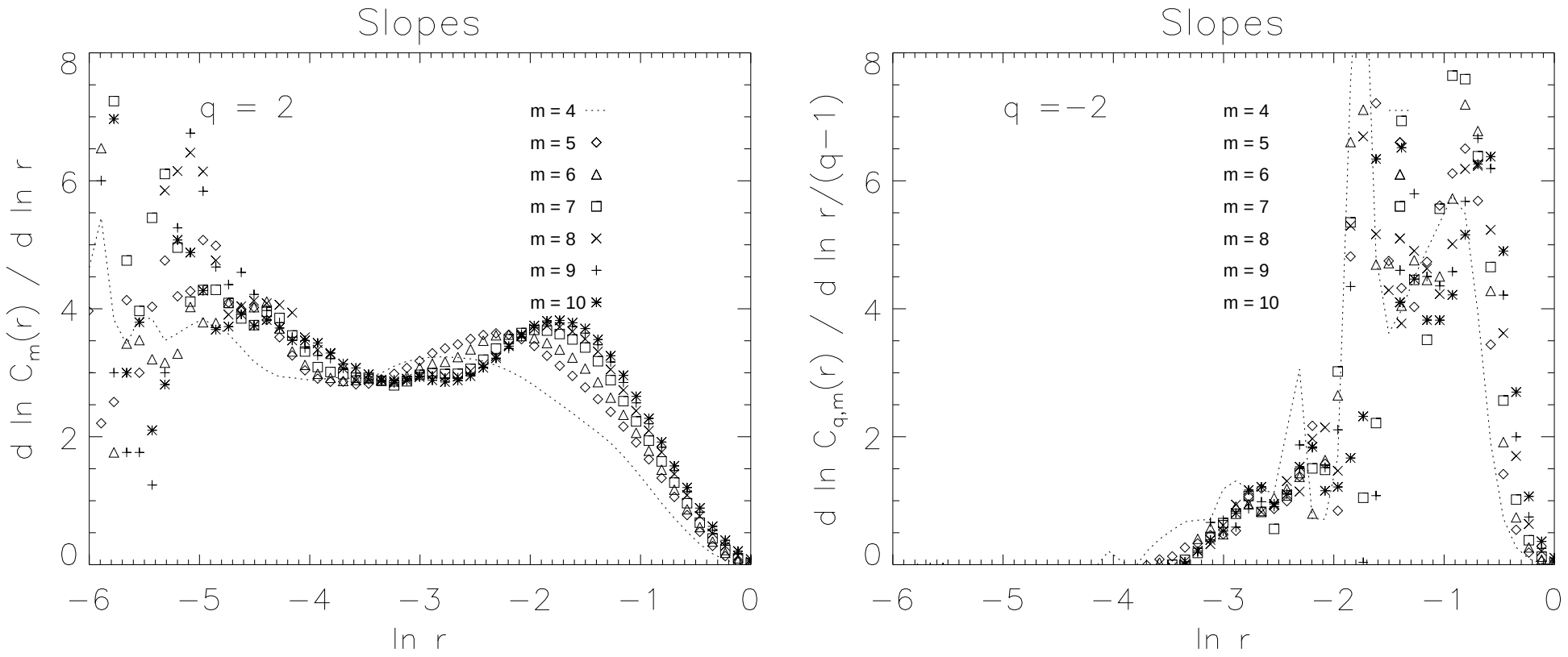

Fig. 5. The slopes $D_{q,m}(r) = \mathrm{d}[\ln C_{q,m}(r)]/\mathrm{d}(\ln r)/(q-1)$ of the generalized correlation sum $C_{q,m}(r)$ versus $\ln r$ (normalized) obtained for detrended and filtered data are shown for various embedding dimensions m for (a) $q = 2$ and (b) $q = -2$, taken from (Macek, 2006).

TABLE 1. Solar wind velocity fluctuations* data	
Number of data points, N	26163
Sampling time, Δt	40.5 s
Skewness†, κ_3	0.59
Kurtosis†, κ_4	0.37
Minimum frequency	9.4 $\times 10^{-7}$ Hz
Dominant frequency	2.5 $\times 10^{-5}$ Hz
Maximum frequency	1.2 $\times 10^{-2}$ Hz
Relative complexity‡	0.1
Autocorrelation time§, t_{a}	7.1 $\times 10^{3}$ s
Correlation dimension¶, D_2	3.35 ± 0.21
Entropy‡¶, $(q = 2), K_2$	0.1
Largest Lyapunov exponent‡¶, $\lambda_{\max}$	1/4 – 1/3
Predictability horizon time‡	3 $\times 10^{4}$ s

*Slow trends (1) $344.596 - 20.291\ t - 0.358\ t^2$, and $88.608 - 452.349\ t + 343.471\ t^2$ (2) $397.847 - 291.602\ t - 241.999\ t^2$, and $-30.050 + 87.756\ t - 77.773\ t^2$ (with t being a fraction of a given sample) were subtracted from the original data, $v(t_i)$ and $v_A(t_i)$, in km s^{-1}, and the data were (8-fold) smoothed using moving averages and singular-value decomposition with five eigenvalues. The resulting range of data $x_{\max} - x_{\min} = 226.4$ km s^{-1}.

†The third and fourth moments of the distribution function are (with average velocity $\langle x \rangle = 0.622$ km s^{-1} and standard deviation $\sigma = 33.514$ km s^{-1})

$$\kappa_3 \ = \ \frac{1}{N} \sum_{i=1}^{N} \left[\frac{x_i \ - \ < x >}{\sigma} \right]^3, \ \ \kappa_4 \ = \ \frac{1}{N} \sum_{i=1}^{N} \left[\frac{x_i \ - \ < x >}{\sigma} \right]^4 \ - \ 3$$

‡Approximately.

§The autocorrelation time t_a is given by $(\langle x(t)x(t+t_{\rm a})\rangle - \langle x(t)\rangle^2)/\sigma^2 = {\rm e}^{-1}$. We take a delay $\tau = t_a = 174\ \Delta t$, which is smaller than the first zero of this function, $1250\ \Delta t$.

¶For large enough m, a plateau in Figs 7 (a) and (b), we have a slope ($q = 2$ in eq. (4))) $D_2 \ \approx \ \frac{\ln\ C_m(r)}{\ln\ (r)}$, where the correlation function is given in eq. (8) The average slope for $6 \leq m \leq 10$ is taken as D_2. Similarly, $K_2 \ \approx \ \frac{1}{3}\ \log_2 \ \left[\ \frac{C_m(r)}{C_{m+3}(r)} \ \right]$ is the $q = 2$ entropy (base 2) in the same units as $\lambda_{\max}$ (bits per data sample), $8 \leq m \leq 10$.

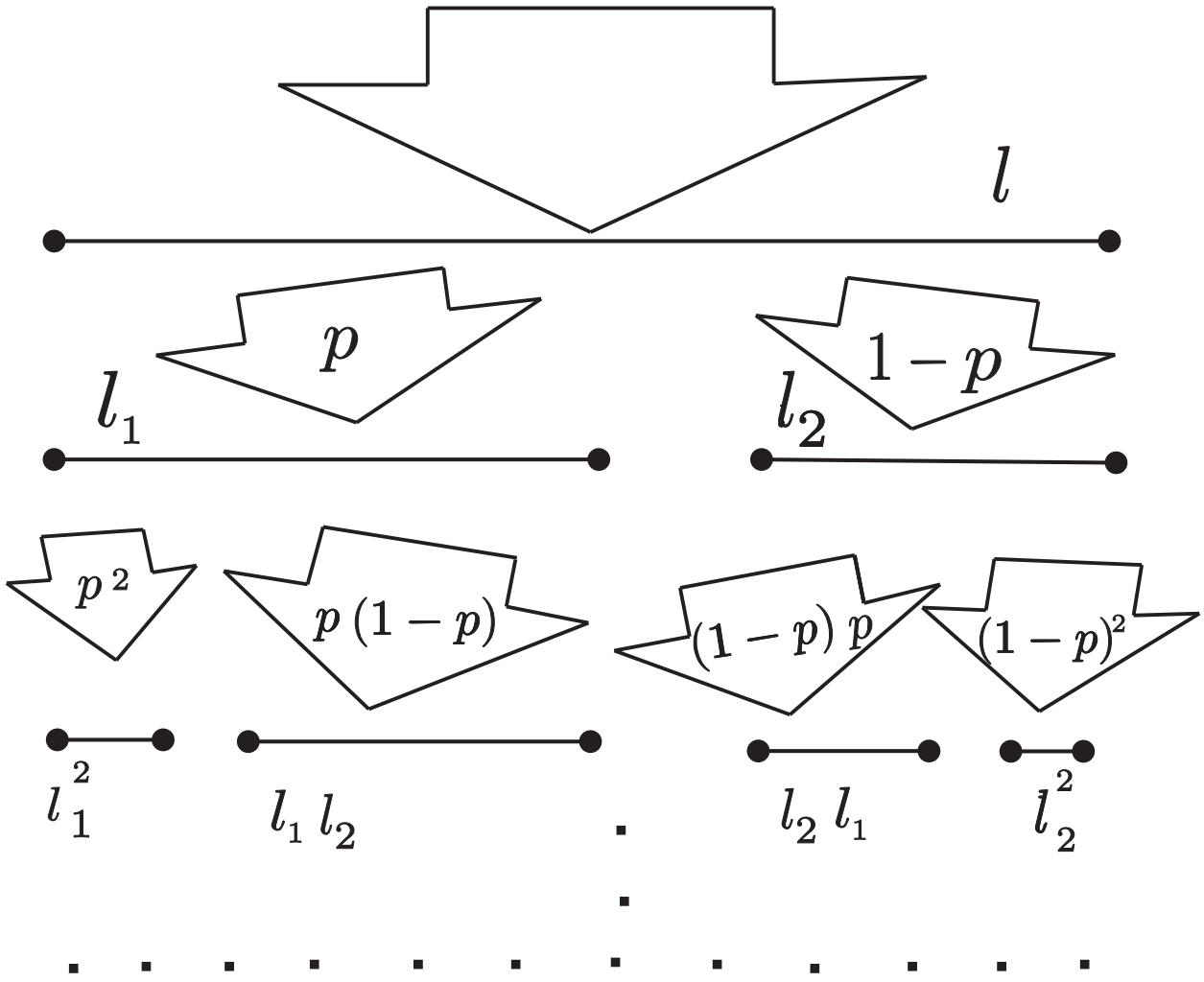

Fig. 6. Generalized two-scale weighted Cantor set model for solar wind turbulence.

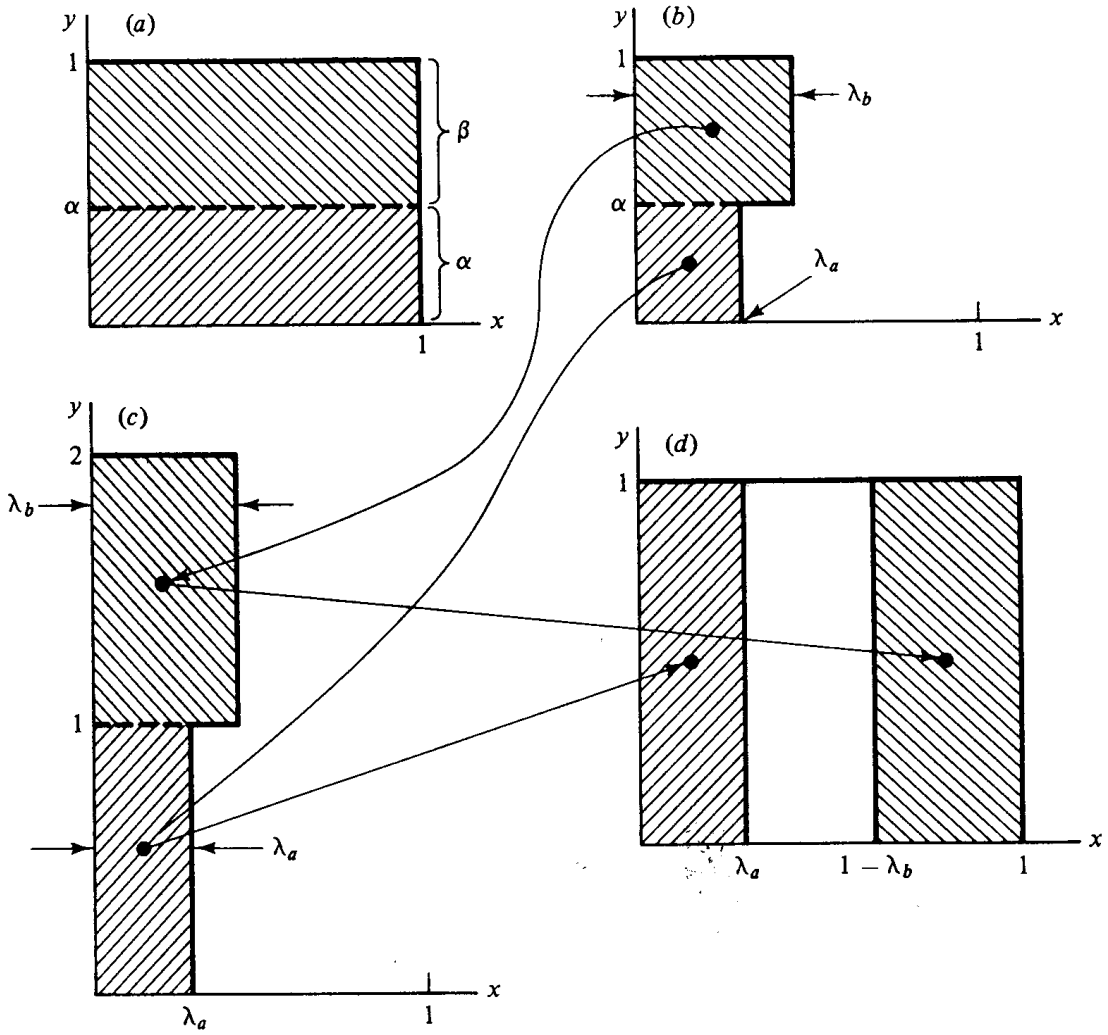

Fig. 7. Action of the generalized baker's map on the unit square.

The generalized self-similar baker's map (Farmer et al., 1983; Ott, 1993):

$$
\begin{aligned}
x_{n+1} &= \begin{cases} l_1 x_n & \text{for } y_n < p \\ (1-l_2) + l_2 x_n & \text{for } y_n \geq p \end{cases} \\
y_{n+1} &= \begin{cases} \frac{y_n}{p} & \text{for } y_n < p \\ \frac{y_n - p}{1-p} & \text{for } y_n \geq p \end{cases}
\end{aligned}
\tag{14}
$$

Parameters:

- $p \leq 1/2$, natural invariant measure on the attractor of the system, the probability of visiting one region of the square (the probability of visiting the remaining region is $1-p$);

- $l_1 + l_2 \leq 1$, folding and dissipation parameters (uniform compression, stretching and folding in the phase space).

Solutions

Transcendental equation

$$p^q \; l_1^{(1-q)D_q} + (1-p)^q \; l_2^{(1-q)D_q} = 1 \tag{15}$$

Legendre transformation

$$\alpha(q) = \frac{\mathrm{d}\,[(q-1)D_q]}{\mathrm{d}q} \tag{16}$$

$$f(\alpha) = q\alpha(q) - (q-1)D_q \tag{17}$$

For $l_1 = l_2 = s$ and any q in Eq. (4) one has for the generalized dimension of the attractor (projected onto one axis)

$$(q-1)D_q = \frac{\ln[p^q + (1-p)^q]}{\ln\, s}. \tag{18}$$

No dissipation ($s = 1/2$):
the multifractal cascade $p-$model for fully developed turbulence,
the generalized weighted Cantor set (Meneveau and Sreenivasan, 1987).
The usual middle one-third Cantor set (without any multifractality):
$p = 1/2$ and $s = 1/3$.

The difference of the maximum and minimum dimension
(the least dense and most dense points on the attractor)

$$D_{-\infty} - D_{+\infty} = \frac{\ln(1/p - 1)}{\ln\,(1/s)} \tag{19}$$

In the limit $p \to 0$ this difference rises to infinity (degree of multifractality).

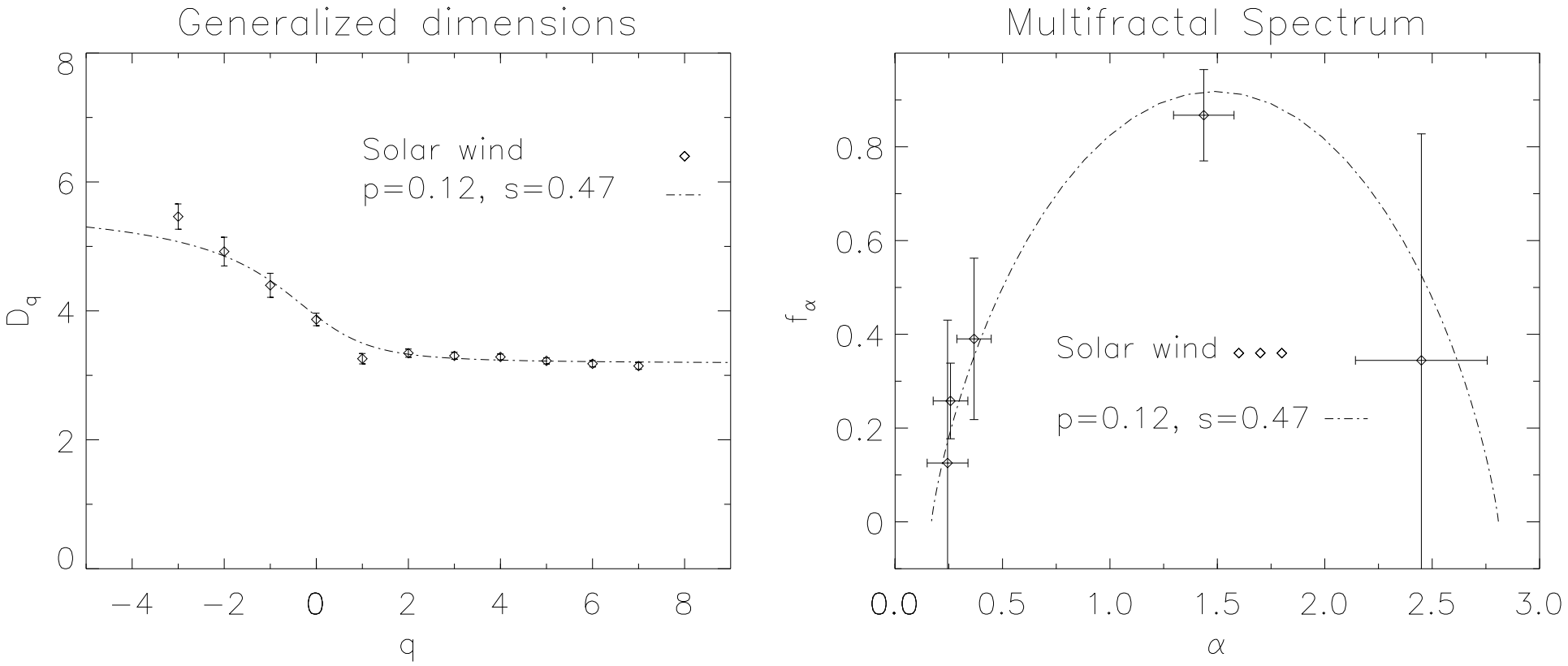

Fig. 8. (a) The generalized dimensions D_q in Equation (4) as a function of q. The correlation dimension is $D_2 = 3.4 \pm 0.1$ (see Table 1). The values of $D_q + 3$ are calculated analytically for the weighted baker's map with $p = 0.12$ and $s = 0.47$ (dashed-dotted line). (b) The singularity spectrum $f(\alpha)$ as a function of α. The values of $f(\alpha)$ projected onto one axis for the weighted baker's map with the same parameters (dashed-dotted line), taken from (Macek, 2006).

The value of parameter p (within some factor) is related to the usual models, which starting from Richardson's version of turbulence, try to recover the observed scaling exponents, which is based on the p-model of turbulence (e.g. Meneveau and Sreenivasan, 1987).

The value of $p = 0.12$ obtained here is roughly consistent with the fitted value in the literature both for laboratory and the solar wind turbulence, which is in the range $0.13 \leq p \leq 0.3$ (e.g., Burlaga, 1991; Carbone, 1993; Carbone and Bruno, 1996; Marsch et al., 1996).

One should only bear in mind that here we take probability measure directly on the solar wind attractor, which quantifies multifractal nonuniformity of visiting various parts of the attractor in the phase space, while the usual p-model is related to the solar wind turbulence cascade for the dissipation rate, which resides in the physical space.

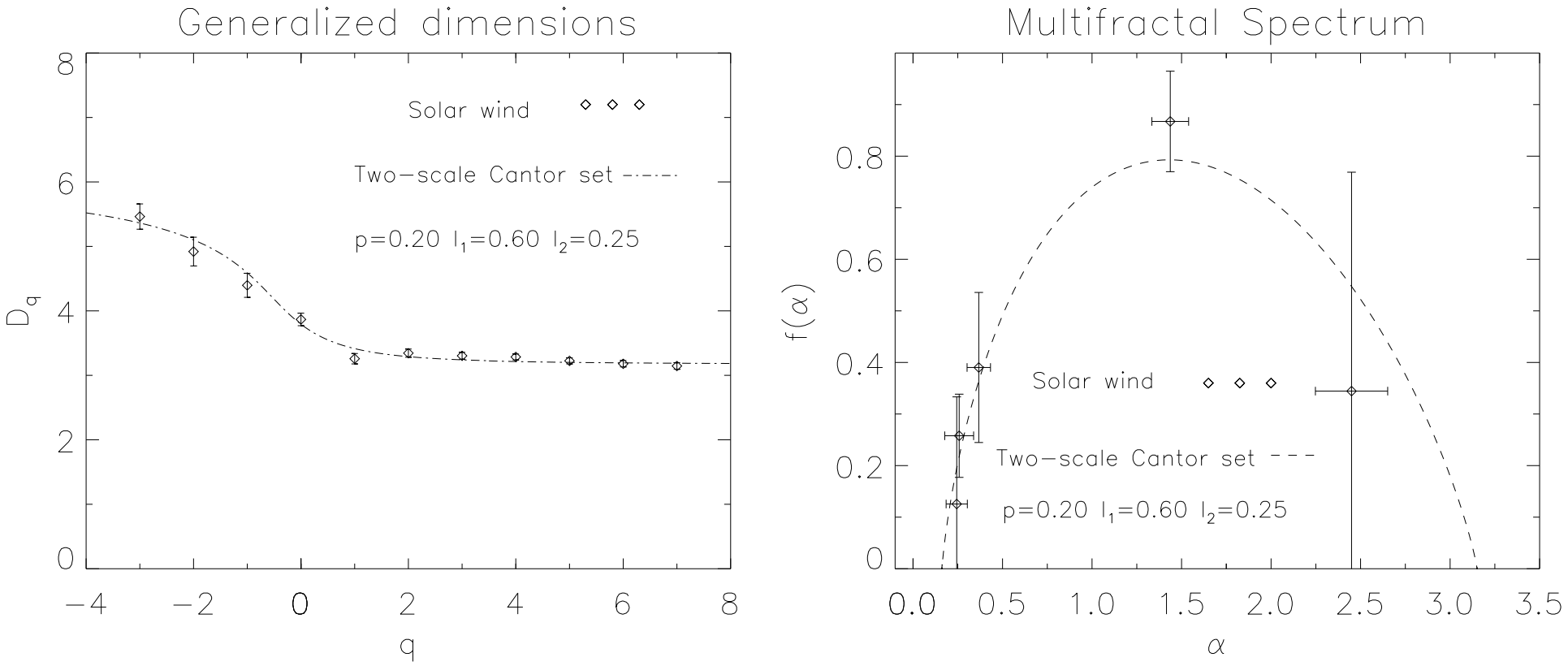

Fig. 9. (a) The generalized dimensions D_q in Equation (4) as a function of q. The values of $D_q + 3$ are calculated analytically for the weighted two-scale Cantor set with $p = 0.20$ and $l_1 = 0.60,\ l_2 = 0.25$ (dashed-dotted line). (b) The singularity spectrum $f(\alpha)$ as a function of α. The values of $f(\alpha)$ projected onto one axis for the weighted two-scale Cantor set with the same parameters (dashed-dotted line).

Conclusions

- The system is likely to have an *attractor* lying in the inertial manifold of low-dimension (probably between three and four).
- We have shown that the singular-value decomposition filter removes some amount of noise, which is sufficient to calculate the generalized dimensions of the solar wind attractor reconstructed in the phase space.
- The obtained multifractal spectrum of this attractor is consistent with that for the multifractal measure on the self-similar weighted baker's map corresponding to the generalized weighted two-scale Cantor set. The action of this map exhibits stretching and folding properties leading to sensitive dependence on initial conditions.
- The values of the parameters fitted demonstrates small dissipation of the complex solar wind dynamical system and shows that some parts of the attractor in phase space are visited at least one order of magnitudes more frequently than other parts.

- We hope that this model could be a useful tool for analysis of the intermittent turbulence in space plasmas. In particular, taking two different scales for eddies in the cascade, one obtains a more general situation than in the usual *p*-model for fully developed turbulence.

Thus our results show multifractal structure of the solar wind in the inner heliosphere.

Hence we suggest that there exists an inertial manifold for the slow solar wind in the inner heliosphere in which the system has *multifractal* structure, and where noise is certainly not dominant.

This means that the observed irregular behavior of the velocity and Alfvénic fluctuations results from intrinsic *nonlinear* dynamics rather than from random external forces.

The multifractal structure, convected by the wind, might probably be related to the complex topology shown by the magnetic field at the source regions of the solar wind.

References

[1] Albano, A. M., Muench, J., Schwartz, C., Mees, A. I., and Rapp, P. E.: 1988, Phys. Rev. A **38**, 3017.

[2] Bruno, R., Carbone, V., Veltri, P., Pietropaolo, E., and Bavassano, B.: 2001, Planet. Space Sci. **49**, 1201.

[3] Burlaga, L. F.: 1991, Geophys. Res. Lett. **18**, 69.

[4] Burlaga, L. F.: 2001, J. Geophys. Res. **106**, 15917.

[5] Carbone, V.: 1993, Phys. Rev. Lett. **71**, 1546.

[6] Carbone, V. and Bruno, R.: 1996, Ann. Geophys. **14**, 777.

[7] Eckmann, J.-P. and Ruelle, D.: 1992, Physica D **56**, 185.

[8] Grassberger, P.: 1983, Phys. Lett. A **97**, 227.

[9] Grassberger P. and Procaccia, I.: 1983, Physica D **9**, 189.

[10] Halsey, T. C., Jensen, M. H., Kadanoff, L. P., Procaccia, I., and Shraiman, B. I.: 1986, Phys. Rev. A **33**, 1141.

[11] Hentschel, H. G. E. and Procaccia, I.: 1983, Physica D **8**, 435.

[12] Macek, W. M.: 1998, Physica D **122**, 254.

[13] Macek, W. M.: 2002, in Boccaletti, S., Gluckman, B.J., Kurths, J., Pecora, L.M., and Spano, M.L. (eds.), *Experimental Chaos*, **622**, American Institute of Physics, New York, p. 74.

[14] Macek, W. M.: 2003, in Velli, M., Bruno, R., and Malara, F. (eds.), *Solar Wind 10*, **679**, American Institute of Physics, New York, p. 530.

[15] Macek W. M. and Redaelli, S.: 2000, Phys. Rev. E **62**, 6496.

[16] Macek W. M., Bruno, R., and Consolini, G.: 2005, Phys. Rev. E **72**, 017202.

[17] Macek W. M., Bruno, R., and Consolini, G.: 2006, Adv. Space Res, **37**, 461–466.

[18] Macek W. M.: 2006, Space. Sci. Rev, **122**, 329–337.

[19] Mandelbrot, B. B.: 1989, in Pure and Applied Geophys., **131**, Birkhäuser Verlag, Basel, p. 5.

[20] Meneveau, C. and Sreenivasan, K. R.: 1987, Phys. Rev. Lett. **59**, 1424.

[21] Marsch, E. and Tu, C.-Y.: 1997, Nonlinear Proc. Geophys. **4**, 101.

[22] Marsch, E., Tu, C.-Y., and Rosenbauer, H.: 1996, Ann. Geophys. **14**, 259.

[23] Ott, E.: 1993, *Chaos in Dynamical Systems*, Cambridge University Press, Cambridge.

[24] Schwenn, R.: 1990, in: Schwenn, R. and Marsch, E. (eds.), *Physics of the Inner Heliosphere*, **20**. Springer-Verlag, Berlin, p. 99.

[25] Theiler, J.: 1986, Phys. Rev. A **34**, 2427.

[26] Theiler, J., Eubank, S., Longtin, A., Galdrikian, B., and Farmer, J. D.: 1992, Physica D **58**, 77.